

Focal Spots of Size $\lambda/23$ Open Up Far-Field Fluorescence Microscopy at 33 nm Axial Resolution

Marcus Dyba and Stefan W. Hell*

High Resolution Optical Microscopy Group, Max-Planck-Institute for Biophysical Chemistry, 37070 Göttingen, Germany
(Received 19 September 2001; published 4 April 2002)

We report spots of excited molecules of 33 nm width created with focused light of $\lambda = 760$ nm wavelength and conventional optics along the optic axis. This is accomplished by exciting the molecules with a femtosecond pulse and subsequent depletion of their excited state with red-shifted, picosecond-pulsed, counterpropagating, coherent light fields. The $\lambda/23$ ratio constitutes what is to our knowledge the sharpest spatial definition attained with freely propagating electromagnetic radiation. The sub-diffraction spots enable for the first time far-field fluorescence microscopy with resolution at the tens of nanometer scale, as demonstrated in images of membranes of *bacillus megaterium*.

DOI: 10.1103/PhysRevLett.88.163901

PACS numbers: 42.30.-d, 41.90.+e, 42.25.-p, 42.79.-e

In 1873 Ernst Abbe discovered that the smallest focal spot of a lens is limited by diffraction to about $\lambda/2n$, with λ denoting the vacuum wavelength of light and n the refractive index [1]. Abbe's discovery put an end to the improvement in the resolution of far-field light microscopy and established a prominent physical problem, known as the "diffraction barrier." Despite the enormous progress brought about by electron, scanning probe, and near-field optical microscopy, the limited resolution has remained an obstacle in many areas of science. Cell biology, for example, depends on focused light for noninvasively probing the cellular interior at the sub- μm scale. Similarly, in lithography and optical data storage efforts are being made to produce smaller spots in a *noncontact* mode.

As with any great physical challenge, the diffraction barrier preoccupied a number of scientists. In 1952 Toraldo di Francia proposed an intriguing concept to produce smaller focal spots [2]. In a theoretical study he showed that with finely tuned pupil filters the light intensity can be diverted away from the focal point to leave a tiny central spot. Unfortunately, the onset of giant side lobes rendered the method impractical. A more straightforward approach has been to reduce λ , as in x-ray-microscopy. Indeed a resolution approaching 30 nm has been reported with this technique [3]. However, abandoning visible light in favor of $\lambda = 2\text{--}4$ nm synchrotron radiation not only adds complexity but is incompatible with live cell studies [3]. Another approach is to enlarge the aperture as realized in 4Pi microscopy [4]: by the coherent addition of the two wave fronts of opposing lenses the resolution along the optic axis has been improved from ~ 500 to ~ 100 nm. However, these concepts are still diffraction limited. A concept which really breaks the diffraction limit in the important imaging by fluorescence is stimulated emission depletion (STED) microscopy [4,5]. Its rationale is to suppress the spontaneous emission at the periphery of the diffraction-limited fluorescence spot of a scanning confocal microscope by stimulated emission. The suppression occurs in such a way that fluorescence is allowed at the focal point, but not in its proximity. The result is a fluores-

cence spot, i.e., an effective point-spread-function (PSF) of the microscope, that is below the diffraction limit [6].

In this work we demonstrate fluorescent spots of 33–46 nm extent produced with $\lambda = 745\text{--}760$ nm and conventional lenses. Moreover, we employ these spots to deliver for the first time far-field microscopy images with resolution on the order of tens of nanometer.

Our result became possible by synergistically implementing elements of the two unrelated concepts of STED and 4Pi microscopy. The fluorescent sample is placed in the common focus of two opposing lenses, but excitation and detection are performed through a single lens, L_1 , only (Fig. 1). For this purpose a train of 250 fs pulses of 554 nm wavelength are directed via mirror M_1 , beam-splitter BS, and the dichroic mirror DC_2 . The lenses, which are alternatively pairs of water or oil immersion lenses, feature the numerical aperture, 1.2 and 1.4, respectively, thereby establishing a tight excitation intensity PSF $h_{\text{exc}}(\vec{r})$ (Fig. 2a). The fluorescence is imaged onto a confocal point detector, described by a detection PSF $h_{\text{det}}(\vec{r})$. We used the styryl dyes RH414 (Molecular Probes, Eugene OR) and Pyridine 2 (Lambda Physik, Göttingen, Germany) emitting in the 600–760 nm range.

Immediately after the excitation, a pulse of $\lambda = 745\text{--}760$ nm and $\tau = 13$ ps duration, denoted by STED pulse, enters the focal region. These photons primarily act on the excited state S_1 , inducing stimulated emission down to a vibrational sublevel of the ground state S_0^{vib} (Fig. 1b). Subpicosecond vibrational decay empties S_0^{vib} , so that repumping into S_1 is largely ineffective. By the time the STED pulse has vanished, the population of the S_1 is $N(t = \tau, h_{\text{STED}}) = N_0 \exp(-k_{fl}\tau - \sigma h_{\text{STED}})$, where N_0 is the population just after excitation, $k_{fl} \approx (1 \text{ ns})^{-1} \ll \tau^{-1}$ is the radiative decay rate, $\sigma \approx 10^{-16} \text{ cm}^2$ the cross section for stimulated emission, and $h_{\text{STED}}(\vec{r})$ is the PSF of the STED pulse in photons per area per pulse. Hence, fluorescence is reduced by $\eta(h_{\text{STED}}) = \int dt \times N(t, h_{\text{STED}}) / \int dt N(t, 0) = \exp(-\sigma h_{\text{STED}})$. (The consideration of a finite vibrational lifetime requires the numerical solution of a set of differential equations, in

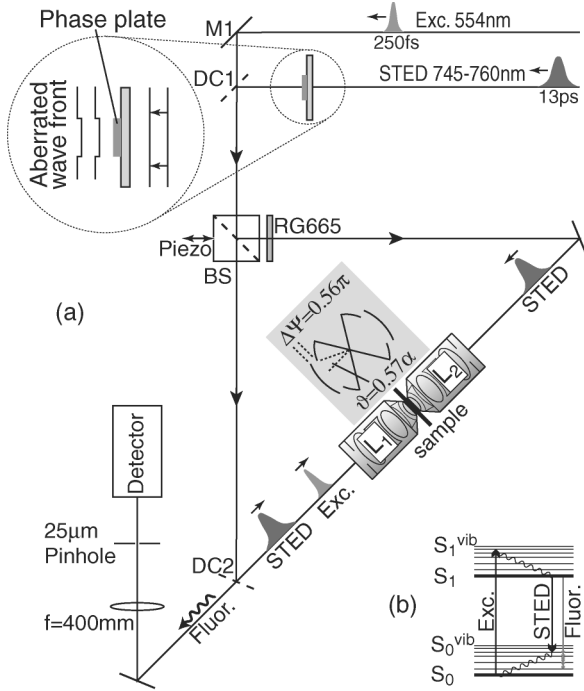


FIG. 1. STED-4Pi microscope. (a) Fluorescence excitation and detection occur via lens L_1 , whereas stimulated emission is generated by the light field of counterpropagating, aberrated wave fronts of L_1 and L_2 . Imaging is accomplished by scanning the sample through the sub-diffraction-sized spot of the two lenses. The inserted sketches depict the aberration induced by the phase plate on the counterpropagating STED-beam wave fronts. (b) Fluorophore energy levels.

which case a slight deviation from the exponential law is found [4].) In Fig. 2d we show the *measured* $\eta(\bar{h}_{\text{STED}})$ for the dyes used, with \bar{h}_{STED} denoting $h_{\text{STED}}(\bar{r})$ averaged over the Airy disk. For $\bar{h}_{\text{STED}} > 10^{16} \text{ cm}^{-2}$ STED is the predominant process with Pyridine 2 and fluorescence is reduced down to 5.5%. The depletion of the membrane-incorporated dye RH414 is less efficient, but still pronounced.

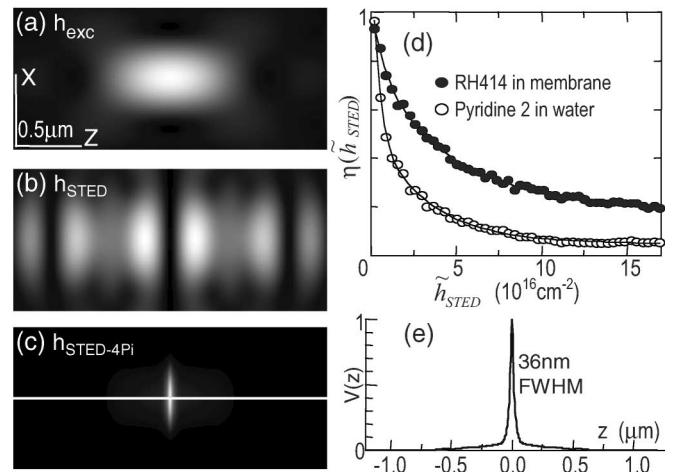


FIG. 2. Calculated intensity point-spread functions for: (a) excitation, (b) stimulated emission, and (c) the effective PSF, i.e., fluorescent spot of the STED-4Pi-microscope. Panel (d) depicts the measured fluorescence as a function of the stimulating photon density. Panel (e) is the calculated response $V(z)$ to an infinitely thin fluorescence plane. (c) and (e) reveal a fundamental improvement of resolution in z .

To reduce the spot size, $h_{\text{STED}}(\bar{r})$ must vanish at the focal point $\bar{r} = 0$ but be high elsewhere. A narrow minimum of $\sim \lambda/(4n)$ full-width-half-maximum (FWHM) is achieved with a standing wave. A planar standing wave, however, exhibits many minima in which fluorescence would be still present. To create a $h_{\text{STED}}(\bar{r})$ with a single minimum, we exploit the high focusing angle and symmetry of the 4Pi microscope. An aberration prior to BS blurs potential side minima, but still renders $h_{\text{STED}}(0) = 0$. Hence, we introduced an aberration $\Psi(\vartheta) = m\pi\theta(\vartheta - P\alpha)$ in the STED beam, whereby $0 \leq \vartheta \leq \alpha$ denotes the semiaperture angle and θ the Heaviside step function. For the oil and water lenses we elected $m_{\text{oil}} = 0.4$, $P_{\text{oil}} = 0.37$ and $m_{\text{water}} = 0.56$, $P_{\text{water}} = 0.57$, respectively, $\Psi(\vartheta)$ was realized by a MgF_2 coated glass plate [6], as depicted in Fig. 1. Destructive phase at $\bar{r} = 0$ was adjusted by a piezo acting on BS. Following the theory by Richards and Wolf [7] we obtain for the focal intensity:

$$h_{\text{STED}}(\bar{r}) = \frac{n^2 c \varepsilon_0 \tau}{2 \hbar \omega} |\vec{E}_1(\bar{r}) + \vec{E}_2(\bar{r})|^2, \quad \text{with } \vec{E}_2(r, z, \phi) = \begin{pmatrix} 1 & 0 & 0 \\ 0 & -1 & 0 \\ 0 & 0 & -1 \end{pmatrix} \vec{E}_1(r, -z, -\phi),$$

$$\vec{E}_1(r, z, \phi) = \frac{-i E_0 n f}{\lambda} \int_0^\alpha d\vartheta d\phi' \sqrt{\cos\vartheta} \sin\vartheta \exp\{i[\Psi(\vartheta) + k(s - f)]\} \times \begin{pmatrix} \cos^2(\phi' - \phi) \cos\vartheta + \sin^2(\phi' - \phi) \\ \sin(\phi' - \phi) \cos(\phi' - \phi) [\cos\vartheta - 1] \\ -\cos(\phi' - \phi) \sin\vartheta \end{pmatrix}, \quad (1)$$

where $\vec{E}_{1,2}$ denotes the electric field amplitude in cylindrical coordinates, E_0 is the pulse-averaged amplitude at the lens entrance pupil, c the speed of light, ε_0 the permittivity of free space, f is the focal length, s the path from the point (f, θ, ϕ) on the converging wave front to (r, z, ϕ) , and $k = 2\pi n/\lambda$. $\Psi(\vartheta)$ an aberration denoting

any phase deviation from a spherical wave front. Figure 2b depicts the numerically calculated $h_{\text{STED}}(r, z, 0)$ featuring the desired central minimum. $h_{\text{exc}}(\bar{r})$ of Fig. 2a and $h_{\text{det}}(\bar{r})$ are gained by setting $\Psi(\vartheta) = 0$ and calculating $|\vec{E}_1(\bar{r})|^2$ for the excitation and fluorescence wavelength, respectively. For excitation and stimulated emission

we assumed x polarization ($\phi = 0$); the detection was unpolarized ($\phi = \pi/4$). Apart from a constant C , the effective PSF and spot size of our STED-4Pi-microscope is now

$$h_{\text{eff}}(\vec{r}) = Ch_{\text{exc}}(\vec{r})h_{\text{det}}(\vec{r})\eta[h_{\text{STED}}(\vec{r})] \\ \cong Ch_{\text{exc}}(\vec{r})h_{\text{det}}(\vec{r})\exp[-\sigma h_{\text{STED}}(\vec{r})]. \quad (2)$$

The exponential suppression by $h_{\text{STED}}(\vec{r})$ squeezes the spot below the diffraction limit. An unbound increase of $h_{\text{STED}}(\vec{r})$ would lead to resolution at the molecular scale. The value achievable with our set of conditions, however, is finite and assessed by implementing the measured $\eta(\vec{h}_{\text{STED}})$ of Fig. 2d into $h_{\text{STED}}(\vec{r})$ of Fig. 2b. The evaluation of $h_{\text{eff}}(\vec{r})$ for $\max(h_{\text{STED}}) = 4 \times 10^{17} \text{ cm}^{-2}$ yields a spot that is fundamentally reduced along the optic axis (Fig. 2c). The associated axial response $V(z) = \iint h_{\text{eff}}(r, z, \phi) r dr d\phi$ features a FWHM of 36 nm (Fig. 2e).

To verify this prediction, we carried out a series of measurements. $V(z)$ was acquired by imaging an axial fluorescence half space, such as the edge of a Pyridine 2 solution and calculating its derivative. Figure 3a shows $V(z)$ for $\max(h_{\text{STED}}) = 7.3 \times 10^{17} \text{ cm}^{-2}$, $\lambda = 760 \text{ nm}$, and oil immersion lenses. The FWHM was $33 \pm 2 \text{ nm}$, in agreement with prediction. Being relevant to biological imaging, we also investigated water immersion. In this case we precipitated a thin ($<10 \text{ nm}$) dye layer on the cover slip out of a dilute aqueous solution of Pyridine 2, so as to establish the z response directly. The $V(z)$ of the STED-4Pi-microscope, recorded at $\max(h_{\text{STED}}) = 3.8 \times 10^{17} \text{ cm}^{-2}$ and $\lambda = 745 \text{ nm}$, FWHM of $46 \pm 5 \text{ nm}$, was narrower than its confocal counterpart by 17.5 ± 2 (Fig. 3b).

At the highest power level, the residual stimulating intensity at $\vec{r} = 0$ led to a 55% reduction of $V(z = 0)$ of the STED-4Pi signal as compared to its confocal counterpart. Figure 3b also reveals that $V(z)$ response exhibited side maxima of 18–24% at $z \approx \pm \lambda_{\text{STED}}/2n$, originating from an incomplete depletion at the side minima of $h_{\text{STED}}(\vec{r})$. Potential remedies are an improved $\Psi(\vartheta)$ and filtering by linear deconvolution. Figure 3c shows xz images of two ultrathin fluorescent layers on cover slips separated by 560 nm. In contrast to the confocal recording the STED-4Pi-microscope separates them clearly.

In a biological imaging application, we labeled the membrane of *bacillus megaterium* with RH414. The dye molecules are incorporated with the transition dipole oriented primarily perpendicular to the membrane [8]. Figure 4a is a standard confocal xz image, revealing that the confocal mode overemphasized the membrane regions oriented in z , partly due to the excitation field being parallel to the transition dipoles, but also to the confocal spot being elongated by a factor of 4 in z . In the STED-4Pi microscope, the situation was inverted. According to the calculation of Fig. 2c, h_{eff} was now 4 times narrower in z . The STED-4Pi-counterpart image of Fig. 4b confirms this since the transverse parts of the

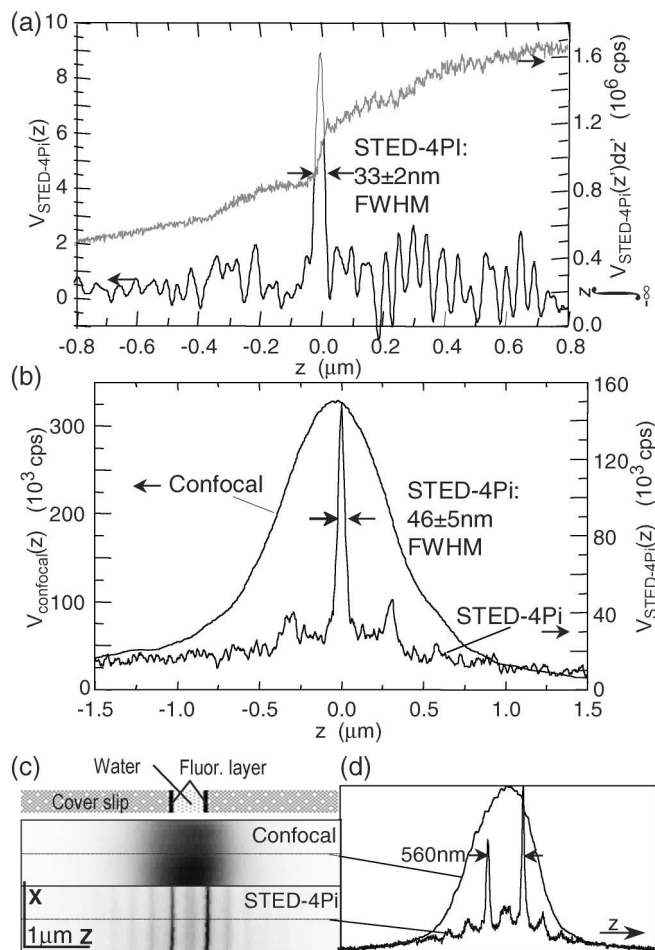


FIG. 3. Z resolution as quantified by the axial response $V(z)$ for (a) oil and (b) water immersion lenses. Note the experimental confirmation of the prediction in Fig. 2(e). Panel (c) compares confocal and STED-4Pi xz images of thin fluorescent layers at 560 nm distance, separated by a dilute watery fluorescence solution: the z profiles are shown in (d). The layers are not distinguishable in the confocal, but clearly in the STED-4Pi microscope.

membrane were more strongly represented. The main result, however, was a vastly improved axial resolution. The image also exhibited side-lobe effects, anticipated from the measured $V(z)$. One reason for the lobes was the incomplete suppression in the side minima; another was the less favorable $\eta(\vec{h}_{\text{STED}})$ for the membrane-incorporated RH414 molecules, as displayed in Fig. 2d. Fortunately, the effect of the lobes can be dealt with a single-step, linear Tikhonov-filter [9] extracted from an experimental $V(z)$ featuring the same lobe height as the bacterial membrane. The resulting image is shown in Fig. 4c. The profiles through the membranes exhibit a 30 nm FWHM and a distinct separation of opposite membrane regions.

The $\max(h_{\text{STED}}) = 5.1 \times 10^{17} \text{ cm}^{-2}$ at $\lambda = 745 \text{ nm}$ was achieved by focusing 8.78 mW of average power, a level well within the range of what is typically used in nonlinear microscopy. It is tempting to target molecular resolution by further increasing $\max(h_{\text{STED}})$, but this

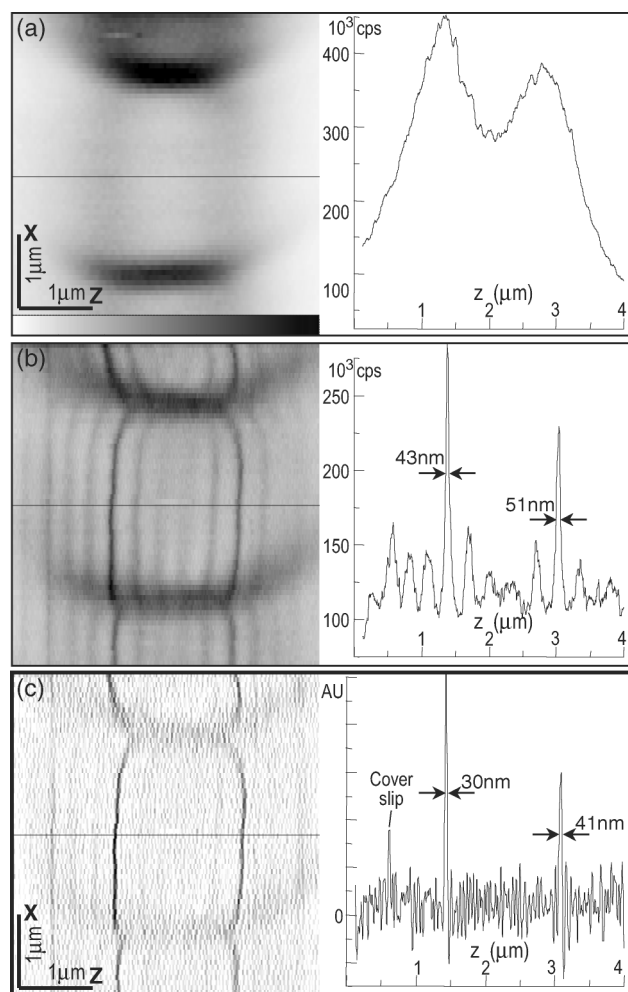


FIG. 4. XZ images of membrane-labeled bacteria: (a) confocal, (b) STED-4Pi, (c) STED-4Pi after linear filtering. (b) and (c) mark the first far-field light microscopy images with spatial resolution of $\sim 30\text{--}40$ nm, corresponding to $\lambda/23$.

endeavor will be challenged by photobleaching and by the residual $h_{\text{STED}}(0) \approx 0$. The latter could possibly be met by implementing active optical elements. Importantly, the STED wavelength and not its excitation partner establish the achievable resolution. Two consequences arise from this fact. First, with a molecular system operating at $\lambda = 380$ nm one should be able to achieve ~ 17 nm. Second, the details of the excitation spot are not important; in fact, our system was optimized only for $\lambda = 745\text{--}760$ nm, which simplifies realization.

The STED-4Pi microscope improves the resolution in the z direction. Evaluation of the intensity profile of a z -oriented bacterial membrane revealed a transverse resolution of 250 ± 10 nm (FWHM), both for the 4Pi-STED and the regular confocal setup. This is in agreement with the FWHM of 234 nm predicted for the utilized water immersion lens. To gain a factor of 3 or more in the transverse direction one can apply an additional STED pulse with a doughnut-shaped $h_{\text{STED}}(\vec{r})$. Consecutive action of both would sculpt the spot laterally and axially so that the

focal volume as defined by the FWHM could be squeezed $\sim 17 \times 3^2 = 153$ -fold.

We note that the xz image in Fig. 4 would not have been possible with near-field optics, because 3D sectioning requires freely propagating waves. We also note that the axial resolution benchmark reported here is on the order of the transverse resolution in x-ray microscopy [3], which, however, requires a 250-fold smaller wavelength.

The strategy by which we break the diffraction barrier is photoinduced saturated depletion of the excited state right in the proximity of a fully unaffected region. This strategy could be applied to any photostable three-level system with a transient state into which the excited molecules are shelved. Therefore possible alternatives to stimulated emission are depletion of the ground state [4] or photoinduced cis-trans isomerization. Our results may also have implications for microlithography and data storage, for which methods are being sought that open up the nanometer scale with visible light. Having defined a ~ 30 nm spot of excited molecules, one could apply a third light field initiating a photochemical reaction with the same resolution.

In summary, we have demonstrated focal spots of excited molecules with 33 nm spatial extent along the optic axis in full-width-half-maximum. Corresponding to $1/23$ of the applied wavelength, this is fundamentally beyond the diffraction limit and constitutes to our knowledge the smallest spatial definition hitherto attained with freely propagating electromagnetic radiation. We have implemented these spots in light microscopy and, using conventionally focused visible and near-infrared light, obtained the first far-field images featuring a resolution of tens of nanometer.

We thank S. Jakobs and T. Klar for valuable discussions. This work was supported by the DFG through Grant No. He-1977.

*Email address: shell@gwdg.de

- [1] E. Abbe, Arch. Mikrosk. Anat. **9**, 413 (1873).
- [2] G. Toraldo di Francia, Nuovo Cimento Suppl. **9**, 426 (1952).
- [3] W. Meyer-Ilse, D. Hamamoto, A. Nair, S. A. Lelievre, G. Denbeaux, L. Johnson, A. L. Pearson, D. Yager, M. A. Legros, and C. A. Larabell, J. Microsc. **201**, 395 (2000).
- [4] S. W. Hell, in *Topics in Fluorescence Spectroscopy*, edited by J. R. Lakowicz (Plenum Press, New York, 1997), Vol. 5, p. 361.
- [5] S. W. Hell and J. Wichmann, Opt. Lett. **19**, 780 (1994).
- [6] T. A. Klar, S. Jakobs, M. Dyba, A. Egner, and S. W. Hell, Proc. Natl. Acad. Sci. U.S.A. **97**, 8206 (2000).
- [7] B. Richards and E. Wolf, Proc. R. Soc. London A **253**, 358 (1959).
- [8] L. Moreaux, O. Sandre, S. Charpak, M. Blanchard-Desce, and J. Mertz, Biophys. J. **80**, 1568 (2001).
- [9] A. N. Tikhonov and V. Y. Arsenin, *Solutions of Ill-Posed Problems* (Wiley, New York, 1977).